Void nucleation as a diffusive instability

Deepak Kumar
Department of Physics, University of Roorkee, Roorkee 247667, Uttar Pradesh, India

Subrata Ray
Department of Metallurgical Engineering, University of Roorkee, Roorkee 247667, Uttar Pradesh, India
(Received 5 August 1985; revised manuscript received 20 June 1986)

The dynamics of vacancies in a system with both production and annihilation mechanisms have been analyzed as to their coalescence to form voids. The modeling of the phenomena is done by introducing a vacancy-concentration field. An equation for this field is formulated which incorporates, in a simplified way, (i) vacancy diffusion, (ii) mutual pairwise interaction among vacancies, (iii) their loss due to mechanisms like recombination with interstitials and absorption at dislocations, grain boundaries, etc., and (iv) their production by incoming radiation. The recombination with interstitials is treated in two schemes. The resulting equations are analyzed for a domain, under the boundary condition that the domain boundaries are perfect sinks. Such a domain should mimic grains in materials. The equations exhibit two kinds of behaviors depending upon the magnitude of the production rate P. If P is below a certain value $P_{\rm th}$, the equations have steady-state solutions which are approached from the initial thermal state. When $P \geq P_{\rm th}$, a coalescence instability occurs in time, which can be thought of as resulting from a negative diffusion coefficient. We have made theoretical estimates of $P_{\rm th}$ in both the schemes which are in very good agreement with numerical calculations.

I. INTRODUCTION

Voids are observed to form in metals and alloys under different physical conditions in which there is a generation of excess vacancies. The formation of voids especially under irradiation is a problem of great technological importance, since voids influence the material properties in a significant way. Much attention has been given to the nucleation and evolution of voids and other extended structures under irradiation conditions[1–5] and during fracture of ductile materials.[6–8]

Since the main motivation behind void studies is the understanding of swelling in irradiated material, many of the earlier studies dealt with the question of growth of voids.[9–11] More recently the interest has also turned towards the mechanisms of nucleation of voids.[12–14] The conventional picture of void nucleation is basically similar to the usual nucleation mechanism occurring at any phase transition, with the difference that with void nucleation one is dealing with a nonequilibrium transition. The fluctuations in the density of excess vacancies cause vacancies to form small aggregates, and these aggregates have to grow beyond a critical size by overcoming a free-energy barrier before they can form voids. The vacancy aggregates are stabilized in a significant way by the presence of inert gases such as He and other impurities.[12–14]

The purpose of the present paper is to examine a situation which arises when the production rate of vacancies is high. It is shown that beyond a critical production rate, the vacancies can coalesce rather spontaneously due to a diffusive instability. The relation of this mechanism to the fluctuation mechanism discussed above is similar to the relation between the formation of a new phase by spinodal decomposition on one hand, and nucleation-growth mechanism on the other. The transition here is a nonequilibrium one, and the instability is caused by the production rate. This approach is also useful as it also contains a natural mechanism for formation of void lattice. In this paper we have not investigated this aspect, but our preliminary investigations in this direction show promise. While our work was being done, the work of Martin[15] was brought to our attention. Martin's formulation is quite similar to ours, but there are many differences in analysis.

II. EQUATION FOR VACANCY FIELD

A. Diffusion and interaction

In order to understand the conditions of void formation, it is important to analyze the dynamics of vacancies, which are generated in excess, for example, as a primary effect of irradiation. The following kinetic processes occur to vacancies.

(i) Vacancies move due to random thermal processes. Such processes can be described to a good approximation as diffusion of vacancies.

(ii) The vacancies move due to mutual forces between them. The pairwise forces between them at short ranges is attractive. This short-ranged force causes the two nearby vacancies to coalesce, as this process results in reduction of surface and elastic energies. There is also a weaker long-ranged interaction which arises due to the overlapping of the strain fields of the two vacancies. We ignore this interaction as it seems secondary to the problem of vacancy coalescence.

(iii) Vacancies are lost with time due to recombination

with defects like interstitials, dislocations, vacancy loops, and grain boundaries.

Clearly the conditions under which voids form or do not form depend upon the competition among these three processes and the production rate. The actual situation in materials is very complicated, as the processes occurring are very inhomogeneous and depend upon the microstructure and geometrical details of macrodefects in the system. Nevertheless, it is clearly interesting to understand the nature of competition between diffusion, which has a tendency to distribute vacancy concentration uniformly, and the attractive forces which bring them together, in the presence of distributed sources and sinks in the system. For this purpose, we analyze the following simple model. We introduce a continuous function $f(\mathbf{r},t)$ denoting the density of vacancies. When such a density is introduced, the length scale of description is much greater than the lattice or vacancy size. One may now write a vacancy current $J(\mathbf{r},t)$:[8]

$$\mathbf{J}(\mathbf{r},t)=-D\nabla f+\mu f(\mathbf{r},t)\mathbf{F}(\mathbf{r},t)\ , \tag{2.1}$$

where D and μ represent diffusion coefficient and mobility of vacancies, respectively, and $\mathbf{F}(\mathbf{r},t)$ is the force on the vacancy at $(\mathbf{r},t)$. This force which arises due to mutual interaction may be written as

$$\mathbf{F}(\mathbf{r},t)=-\int \nabla V(\mathbf{r}-\mathbf{r}')f(\mathbf{r}',t)d^3r'\ , \tag{2.2}$$

where $V(\mathbf{r}-\mathbf{r}')$ is the mutual potential energy between vacancies at $\mathbf{r}$ and $\mathbf{r}'$.

The dynamical equation for $f(\mathbf{r},t)$ can now be written as

$$\frac{\partial f(\mathbf{r},t)}{\partial t}+\nabla\cdot\mathbf{J}(\mathbf{r},t)=-l(\mathbf{r},t)+P(\mathbf{r},t)\ , \tag{2.3}$$

where $l(\mathbf{r},t)$ and $P(\mathbf{r},t)$ are the rates at which vacancies per unit volume are lost and produced, respectively, around $(\mathbf{r},t)$. The loss term $l(\mathbf{r},t)$ requires a detailed discussion, which we defer to the next section, apart from one point. One of the factors contributing to the loss term is the grain boundaries. We assume that the grain boundaries act as perfect sinks for the vacancies and incorporate their absorption through the boundary condition $f(\mathbf{r},t)=0$, when $\mathbf{r}$ lies on the surface of the grain. The production rate $P(\mathbf{r},t)$ is proportional to the intensity I of the impinging radiation, and can be well assumed to be uniform within a domain or grain. On substituting Eq. (2.1) into Eq. (2.3), the latter takes the form

$$\frac{\partial f(\mathbf{r},t)}{\partial t}+l(\mathbf{r},t)=P+D_v\nabla^2 f+\mu\nabla\cdot\left[f(\mathbf{r},t)\int\nabla V(\mathbf{r}-\mathbf{r}')f(\mathbf{r}',t)d^3r'\right]\ . \tag{2.4}$$

We now consider the situation for a single grain. The last term of the equation can be simplified considerably by exploiting the fact that $V(\mathbf{r}-\mathbf{r}')$ is a short-ranged potential. For study of coalescence, we ignore the long-ranged part of the potential. The integral in the last term of the Eq. (2.4) can be written as

$$\begin{aligned}\int\nabla V(\mathbf{r}-\mathbf{r}')f(\mathbf{r}',t)d^3r'&=-\int\nabla' V(\mathbf{r}-\mathbf{r}')f(\mathbf{r}',t)d^3r'\\&=\text{surface term}+\int V(\mathbf{r}-\mathbf{r}')\nabla' f(\mathbf{r}',t)d^3r'\ .\end{aligned} \tag{2.5}$$

The surface term vanishes due to the boundary condition that $f(\mathbf{r},t)=0$ when $\mathbf{r}$ lies on the surface. Due to the short-ranged property of the potential, we can carry out a Taylor-series expansion for $\nabla' f(\mathbf{r}',t)$ about $\mathbf{r}$ in Eq. (2.5) to write

$$\int\nabla V(\bar{r}-\bar{r}')f(\mathbf{r}',t)d^3r'=\int d^3r'\,V(\mathbf{r}-\mathbf{r}')\{\nabla f(\mathbf{r},t)+[(\mathbf{r}'-\mathbf{r})\cdot\nabla]\nabla f(\mathbf{r})+\tfrac{1}{2}[(\mathbf{r}'-\mathbf{r})\cdot\nabla]^2\nabla f(\mathbf{r},t)+\cdots\}\ . \tag{2.6}$$

To consider coalescence, we shall just keep the first term of the expansion which seems most essential. The second term vanishes automatically if the potential is isotropic. The role of the third term involving third-order derivatives in the current is under investigation, which we do not report here. Further, we write

$$V_0\Omega_i=\int d^3r'\,V(\mathbf{r}-\mathbf{r}')\ , \tag{2.7}$$

where V_0 is a measure of the strength of interaction and Ω_i is a measure of the volume over which the interaction occurs. For a finite domain, the right-hand side (rhs) of the Eq. (2.7) is not independent of $\mathbf{r}$ for points $\mathbf{r}$ close to the surface. However, for a short-ranged potential this introduces insignificant error, being of order $\Omega_i^{1/3}/R$, where R is the linear size of the domain. Substituting these simplifications in Eq. (2.4) and using the Einstein relation to write $\mu=D/k_BT$, we get

$$\frac{\partial f}{\partial t}+l(\mathbf{r},t)=P+D\nabla^2\left[f-\frac{V_0\Omega_i}{2k_BT}f^2\right]\ . \tag{2.8}$$

B. The loss terms

Apart from absorption from grain boundaries, which was considered in the preceding section, the vacancies are lost by two more mechanisms: (a) absorption due to macrodefects such as dislocations, vacancy loops, etc., and (b) recombination with interstitials. The loss rate arising due to absorption by macrodefects is simply proportional to the vacancy concentration and can be written as $k_0 f(\mathbf{r},t)$. In principle, k_0 is also a function of position, being dependent on the configuration of microdefect. But in the spirit outlined above, we take it to be a constant, given by[16,17]

$$k_0 = K_{vs} C_s = \frac{4\pi r_{vs} D_v C_s}{\Omega_a} \tag{2.9}$$

where C_s is the number of macrodefects per atomic volume, r_{vs} is the absorption length characterizing the interaction between vacancies and macrodefects, and Ω_a is the volume of the unit cell in the solid. If one assumes this absorption to be dominated by dislocations, then $4\pi r_{vs} C_s/\Omega_a = \rho_d$, where ρ_d is the number of dislocation lines per unit area. In this case $k_0 = \rho_d D_v$.

The loss rate corresponding to recombination with interstitials can be written as $k_{iv} f(\mathbf{r},t) n(\mathbf{r},t)$, where $n(\mathbf{r},t)$ is the interstitial concentration and

$$k_{iv} = 4\pi r_{iv}(D_i + D_v) , \tag{2.10}$$

where D_i is the diffusion constant for interstitials, and r_{iv} is the absorption length characterizing the vacancy-interstitial interaction. Since $n(\mathbf{r},t)$ is a space- and time-dependent quantity, also being driven by the irradiation, one should in principle write down an equation for $n(\mathbf{r},t)$, incorporating the production, loss, and diffusion of interstitials, in a manner similar to that of the vacancy field. Then one would have to solve two coupled partial differential equations simultaneously. In view of the complexity of the problem and the computational labor involved, we propose to handle the problem in a simpler way, which we believe is reasonably justified under certain circumstances.

The circumstance which we wish to exploit, and which is obtained frequently in practical situations of interest, is the following. In many materials of nuclear interest, the interstitial diffusion is much faster than the vacancy diffusion.[5,18] For example, in iron the hopping activation energy for vacancies is approximately 0.8 eV, whereas that for interstitials it is of order 0.1 eV. This implies that the interstitial diffusion constant D_i is bigger than the vacancy diffusion constant by 12 orders of magnitude at 300 K. This rapid interstitial diffusion allows us to make the following approximations. Firstly we assume that the interstitial concentration reaches a value which is in local equilibrium with the vacancy concentration, i.e., $n(\mathbf{r},t)$ varies adiabatically with vacancy concentration. Another similar consequence of this approximation is that the vacancy-interstitial recombination process is also not affected by vacancy diffusion—which again occurs in a local way and on a time scale faster than the vacancy diffusion. Thus the recombination process can be adequately described in terms of simple rate equations, which also enable us to express $n(\mathbf{r},t)$ in terms of $f(\mathbf{r},t)$. The rate equations are[16,17]

$$\frac{\partial f(\mathbf{r},t)}{\partial t} = P - k_{iv} f(\mathbf{r},t) n(\mathbf{r},t) - k_0 f(\mathbf{r},t) , \tag{2.11}$$

$$\frac{\partial n(\mathbf{r},t)}{\partial t} = P - k_{iv} f(\mathbf{r},t) n(\mathbf{r},t) - K_{is} C_s n(\mathbf{r},t) , \tag{2.12}$$

where

$$K_{is} C_s = \frac{4\pi r_{is} D_i C_s}{\Omega_a} \simeq \frac{4\pi r_{vs} D_i C_s}{\Omega_a} = \frac{D_i}{D_v} k_0 . \tag{2.13}$$

Since in the equation for $n(\mathbf{r},t)$ the slowest time dependence comes from variation of $f(\mathbf{r},t)$, the adiabatic approximation means that $f(\mathbf{r},t)$ can be regarded as time-independent relative to other terms. Allowing this, the solution for $n(\mathbf{r},t)$ can be written down to be

$$n(\mathbf{r},t) = \frac{P}{\gamma} + n(\mathbf{r},0) e^{-\gamma t} , \tag{2.14}$$

where,

$$\gamma = k_{iv} f(\mathbf{r},t) + \frac{D_i}{D_v} k_0 . \tag{2.15}$$

Further, the transient is ignored as $\gamma \gg 1$, and

$$n(\mathbf{r},t) = \frac{P}{k_{iv} f(\mathbf{r},t) + D_i k_0 / D_v} \tag{2.16}$$

$$= \frac{P}{D_i [4\pi r_{iv} f(\mathbf{r},t) + \rho_D]} , \tag{2.17}$$

where (2.17) follows if absorption by only dislocation is considered. We can now write the complete loss term,

$$l(\mathbf{r},t) = k_0 f(\mathbf{r},t) + k_{iv} f(\mathbf{r},t) n(\mathbf{r},t) \tag{2.18}$$

$$= \left[k_0 + \frac{P}{f(\mathbf{r},t) + A} \right] f(\mathbf{r},t) , \tag{2.19}$$

where

$$A = \frac{k_0 D_i}{k_{iv} D_v} = \frac{\rho_d}{4\pi r_{iv}} . \tag{2.20}$$

Note that even after these simplifications, the loss term due to recombination is nonlinear in f and depends upon the production rate P.

Substitution of Eq. (2.19) into Eq. (2.8) completes the derivation of the equation for the vacancy field. For numerical work, and for comparison with other papers in the field, it is convenient to work with the dimensionless variable $C(\mathbf{r},t) = \Omega_a f(\mathbf{r},t)$. We write our final equation in terms of $C(\mathbf{r},t)$ as

$$\frac{\partial}{\partial t} C(\mathbf{r},t) + \left[k_0 + \frac{\tilde{P}}{\tilde{A} + C(\mathbf{r},t)} \right] C(\mathbf{r},t) = \tilde{P} + D_v \nabla^2 \left[C(\mathbf{r},t) - \frac{V_0 \alpha}{2 k_B T} C^2(\mathbf{r},t) \right] , \tag{2.21}$$

where $\tilde{P} = \Omega_a P$, $\alpha = \Omega_i / \Omega_a$, and

$$\tilde{A} = \Omega_a A = \rho_d / (4\pi r_{iv} / \Omega_a) . \tag{2.22}$$

The following sections are devoted to analytical and numerical analyses of Eq. (2.21), for a domain of finite linear size R with the boundary condition $C(\mathbf{r},t) = 0$ at the boundaries.

III. SOLUTION OF THE EQUATION

The basic equation (2.21) that we wish to solve has two kinds of nonlinearities, one in the loss term and the other in the interaction term. We find a lot of insight can be

gained if we consider them separately, before we analyze these nonlinearities together. In the following sections we follow this approach.

A. Diffusive instability due to the interaction term

For purposes of analyzing the diffusive instability due to the interaction term, we ignore for the moment the nonlinearity due to combination with interstitials and consider the equation

$$\frac{\partial}{\partial t}C(\mathbf{r},t)+kC(\mathbf{r},t) = \tilde{P}+D_v\nabla^2\left[C(\mathbf{r},t)-\frac{V_0}{2k_BT}\frac{\Omega_i}{\Omega_a}C^2(\mathbf{r},t)\right], \quad (3.1)$$

where k is some average P-independent effective loss rate. It can be easily seen that this equation has two very different kinds of behaviors, depending upon the value of $\tilde{P}$. Physically P governs the magnitude of f and when f is large, mutual attractive interactions amongst vacancies dominate and at some stage these overcome the diffusive tendencies to cause coalescence. Mathematically, we can easily demonstrate it for an infinite grain. For an infinite grain the steady-state solution of the equation is $C(\mathbf{r},t)=\tilde{P}/k$. Thus we write

$$C(\mathbf{r},t)=\tilde{P}/k+e^{-kt}g(\mathbf{r},t)\ . \quad (3.2)$$

The resulting equation for g is

$$\frac{\partial g}{\partial t}=D_v\left[1-\frac{V_0\alpha}{k_BT}\frac{\tilde{P}}{k}\right]\nabla^2 g-\frac{D_vV_0}{2k_BT}e^{-kt}\nabla^2 g^2\ . \quad (3.3)$$

If we treat g as a perturbation over steady-state solution, or consider times $g\ll\tilde{P}/ke^{kt}$, the second term of the rhs of Eq. (3.3) can be ignored and we note that an effective diffusion coefficient,

$$D_{\text{eff}}=D_v\left[1-\frac{V_0\alpha}{k_BT}\frac{\tilde{P}}{k}\right], \quad (3.4)$$

becomes negative when

$$\tilde{P}>P_{\text{th}}=\frac{k_BT}{V_0\alpha}k\ . \quad (3.5)$$

We see here that above a certain production rate the diffusive tendency is reversed due to interaction. This leads to flow of vacancies from lower concentration to higher concentrations, and we identify this rate as the threshold production rate for the spontaneous formation of voids. Below this rate, the simple diffusion dominates and voids can form only by a nucleation and growth mechanism. These general features have been confirmed by numerical calculations in one dimension, as will be discussed in Sec. IV.

The production rate derived here has a simple physical basis. It is directly proportional to loss rate k and the temperature T, and inversely proportional to coalescence energy V_0. This is so because k controls the average concentration in the system and the larger k is, the larger a value of P is needed to reach the concentration when coalescence can take place. The ratio k_BT/V_0 is essentially the ratio between diffusive mobility which opposes coalescence and the attractive energy which favors coalescence. However, the above considerations are valid only for infinite grain. For finite grains the diffusion causes an additional loss of vacancies at the boundaries of the grain. Qualitatively, one can see that for finite grains $P_{\text{th}}(R)$ will be bigger than that given in (2.5) due to additional loss. The diffusive loss at the boundaries must cause the k factor in Eq. (3.5) to be modified through a function of the form $S(L/R)$, where L is diffusive length given by $(D_v/k)^{1/2}$ and R is the linear size of the grain. This is so because L is roughly the distance a vacancy moves between its creation and extinction. Thus the diffusive loss occurs only for those vacancies which are produced within a distance L from the boundaries. This means that the overall effective extinction rate is affected through a function of the ratio L/R. A more detailed analysis of this finite-size effect is carried out in the next section.

B. Diffusive loss at the boundaries

To do this part of the analysis it is convenient to define new time and length scales

$$t\rightarrow kt \text{ and } \mathbf{r}\rightarrow\mathbf{r}/L\ , \quad (3.6)$$

We first consider the solution of the linear problem

$$\frac{\partial C}{\partial t}+C=\tilde{P}/k+\nabla^2 C\ . \quad (3.7)$$

The solution can be written

$$C=F_T(\mathbf{r},t)+\frac{\tilde{P}}{k}S(\mathbf{r})\ , \quad (3.8)$$

where $S(\mathbf{r})$ is the steady-state solution reached in the $t\rightarrow\infty$ limit. Both F and S can be expanded in the normalized eigenfunctions of the ∇^2 operator with appropriate boundary conditions. If $\psi_n(r)$ and ϵ_n denote such eigenfunctions and eigenvalues,

$$F_T(\mathbf{r},t)=\sum_n\left[A_n-\frac{P_n}{k(1+\epsilon_n)}\right]\psi_n(\mathbf{r})e^{-(1+\epsilon_n)t} \quad (3.9)$$

and

$$\frac{\tilde{P}}{k}S(\mathbf{r})=\sum_n\frac{P_n}{k(1+\epsilon_n)}\psi_n(\mathbf{r})\ , \quad (3.10)$$

where

$$A_n=\int_V f(\mathbf{r},0)\psi_n(\mathbf{r})d^3r \quad (3.11)$$

and

$$P_n=\tilde{P}\int_V\psi_n(\mathbf{r})d^3r\ . \quad (3.12)$$

To analyze the nonlinear equation, we make the substitution

$$C(\mathbf{r},t)=F_T(\mathbf{r},t)g(\mathbf{r},t)+\frac{\tilde{P}}{k}S(\mathbf{r}) \tag{3.13}$$

and find

$$\frac{\partial g}{\partial t}-\frac{2}{F_T}\nabla F_T\cdot\nabla g-\nabla^2 g=-\frac{V_0\alpha}{k_BT}\frac{1}{F_T}\nabla^2(F_T S g)\frac{\tilde{P}}{k}-\frac{V_0\alpha}{2k_BT}\frac{1}{F_T}\nabla^2(F_T^2 g^2)\,. \tag{3.14}$$

Now if we make the approximation that $|\nabla F_T|/F_T$ is small we arrive at the equation

$$\frac{\partial g}{\partial t}=\left[1-\frac{V_0\alpha}{k_BT}\frac{\tilde{P}}{k}\overline{S(\mathbf{r})}\right]V^2 g-\frac{V_0\alpha}{2k_BT}V^2[g^2F_T+g(S-\bar{S})]\,, \tag{3.15}$$

where $\bar{S}$ is the value of $S(\mathbf{r})$ averaged over the domain. Ignoring the nonlinear terms as before we expect the effective diffusion coefficient to go negative, when

$$\frac{\tilde{P}}{k}\overline{S(\mathbf{r})}>\frac{k_BT}{V_0\alpha}\,. \tag{3.16}$$

For a grain of simple geometry, $S(\mathbf{r})$ can be easily calculated. For a cubic grain,

$$S(\mathbf{r})=\left[\frac{4}{\pi^2}\right]^3\sum_{n_1,n_2,n_3}{}'\frac{\sin(n_1\pi x/R)\sin(n_2\pi y/R)\sin(n_3\pi z/R)}{n_1n_2n_3[1+(\pi^2/R^2)(n_1^2+n_2^2+n_3^2)]} \tag{3.17}$$

and

$$\bar{S}=\left[\frac{8}{\pi^2}\right]^3\sum_{n_1,n_2,n_3}{}'\frac{1}{n_1n_2n_3[1+(\pi^2/R^2)(n_1^2+n_2^2+n_3^2)]}\,, \tag{3.18}$$

where a prime on the summation implies that n_1, n_2, and n_3 take only odd integral values. The summation in Eq. (3.18) can be easily done for a one-dimensional domain and we find the threshold rate $P_{\rm th}$ for a one-dimensional domain to be

$$P_{\rm th}/k=\frac{k_BT}{V_0\alpha}\frac{1}{1-(2L/R)\tanh(R/2L)}\,. \tag{3.19}$$

For large R, we have also made an approximate evaluation of Eq. (3.18) and this yields

$$P_{\rm th}/k=\frac{k_BT}{V_0\alpha}\frac{1}{1-(6L/R)\tanh(R/2L)}\,. \tag{3.20}$$

The explicit analysis can also be made for a spherical grain, for which one finds

$$P_{\rm th}/k=\frac{k_BT}{V_0\alpha}\frac{1}{1-(3L/R)[\coth(R/L)-L/R]}\,. \tag{3.21}$$

As expected, $P_{\rm th}$ is found to be a decreasing function of R, because the larger the R is, the smaller is the loss to domain boundaries and consequently the smaller is the production rate required to cause coalescence.

Note that our estimates from Eq. (3.16) are upper bounds for $P_{\rm th}$. The reason is that the coalescence instability occurs at the center of domain, where the vacancy concentration is maximum. This suggests that a better estimate of $P_{\rm th}$ can be obtained by using $S(0)$ in place of $\bar{S}$, i.e., at the threshold

$$\frac{P_{\rm th}}{k}\frac{V_0\Omega}{k_BT}S(0)=1\,. \tag{3.22}$$

This yields

$$P_{\rm th}/k=\begin{cases}\dfrac{k_BT}{V_0\alpha}\dfrac{1}{1-\mathrm{sech}(R/2L)} & \text{for one-dimensional grain} \quad (3.23)\\[2ex] \dfrac{k_BT}{V_0\alpha}\dfrac{1}{1-(L/R)\sinh(R/L)} & \text{for spherical grain}\,. \quad (3.24)\end{cases}$$

The R dependence of $P_{\rm th}$ is also studied numerically, and it will be described in Sec. IV. The numerical results broadly confirm the theoretical picture.

C. Role of interstitial-vacancy recombination

For the considerations of this section, we paraphrase the results of the previous two sections in the following way. The coalesance instability occurs when the production term is large enough to drive the steady concentration in the middle of the grain, $C_s(0)$, to a value $C_{\rm th}$, given by

$$C_{\rm th}=\frac{k_BT}{V_0\alpha}\,. \tag{3.25}$$

In the presence of a linear loss term, the concentration

$C_s(0)$ is related to the production rate through the relation

$$C_s(0)=\frac{\tilde{P}}{k}S(0)\ . \tag{3.26}$$

Thus when P becomes large enough such that $C_s(0)>C_{\rm th}$, the diffusive instability occurs. The primary effect of the loss term arising due to recombination with interstitials [Eq. (2.19)] is to alter the relation given in Eq. (3.26). To see this, we consider how local concentrations build up in the middle of the grain. Since the concentration profile is very flat in the middle, we ignore diffusion and study this build up using rate equations. By using the adiabatic approximation, the rate equation for $C(0,t)$ is

$$\frac{\partial C(0,t)}{\partial t}=\tilde{P}-\left[k_0+\frac{\tilde{P}}{\tilde{A}+C(0,t)}\right]C(0,t)\ . \tag{3.27}$$

The solution for this equation is

$$\left[1+\frac{\tilde{A}}{2\beta}\right]\ln\left[\frac{\beta-\tilde{A}/2-C(0,t)}{\beta-\tilde{A}/2-C(0,0)}\right]+\left[1-\frac{\tilde{A}}{2\beta}\right]\ln\frac{\beta+\tilde{A}/2+C(0,t)}{\beta+\tilde{A}/2+C(0,0)}=-2k_0t\ , \tag{3.28}$$

where

$$\beta=\left[\frac{\tilde{P}\tilde{A}}{k_0}+\frac{\tilde{A}^2}{4}\right]^{1/2}\ . \tag{3.29}$$

This equation implies a monotonic build up of concentration to a steady-state value,

$$C_s(0)=\left[\frac{\tilde{P}\tilde{A}}{k_0}+\frac{A^2}{4}\right]^{1/2}-\frac{A}{2}\ , \tag{3.30}$$

provided that the initial concentration $C(0,0)<C_s(0)$. The quantity $\tilde{A}$ is typically very small. From Table I one can see that for steel, $\tilde{A}\sim 10^{-5}$–10^{-6}, whereas in the vicinity of the threshold, $\tilde{P}\approx 10^{-3}$. Under these conditions, we take $C_s(0)=(\tilde{P}\tilde{A}/k_0)^{1/2}$ and the solution (3.28) can be written as

$$C(0,t)=\left[\frac{\tilde{P}\tilde{A}}{k_0}-Be^{-2k_0t}\right]^{1/2}\ , \tag{3.31}$$

where B is a constant related to the initial concentration. Note that the P dependence of $C_s(0)$ is now very different from the earlier one [see Eq. (3.26)]. This gives rise to rather drastic changes in the estimate of the production threshold for coalescence. Setting $C_s(0)$ from Eq. (3.30) equal to $C_{\rm th}$, one finds $P_{\rm th}$ to be given by

$$\left[\frac{P_{\rm th}\tilde{A}}{k_0}+\frac{\tilde{A}^2}{4}\right]^{1/2}-\frac{\tilde{A}}{2}=\frac{k_BT}{V_0\alpha}\ . \tag{3.32}$$

To account for diffusive loss of vacancies for finite grains, we note that this mainly occurs in the neighborhood of the boundaries, where the vacancy concentration is small, and presumably the nonlinear effects are also small. Thus, the estimates of Sec. III B are approximately correct, and we modify Eq. (3.32) in the following way:

$$\left[\frac{P_{\rm th}\tilde{A}}{k_0}+\frac{\tilde{A}^2}{4}\right]^{1/2}-\frac{\tilde{A}}{2}=\frac{k_BT}{V_0\alpha}\frac{1}{S(0)}\ , \tag{3.33}$$

which in the limit of small A yields

$$\frac{P_{\rm th}}{k_0}=\frac{1}{A}\left[\frac{k_BT}{V_0\alpha}\frac{1}{S(0)}\right]^2\ . \tag{3.34}$$

It might be mentioned at this stage, that when the vacancy-interstitial recombination mechanism is the dominant loss mechanism, i.e., $\tilde{A}$ is small, the production threshold of Eq. (3.34) can also be arrived at, through other related approximation schemes. For example, one might assume that due to fast diffusion, the interstitials reach a quasi-steady-state, in which one finds (using rate equations)

$$n=\frac{D_v}{D_i}f\ . \tag{3.35}$$

Now we allow for the slower variation of f and write the loss term as

$$\begin{aligned} l(\mathbf{r},t)&=k_0f(\mathbf{r},t)+\frac{k_{iv}D_v}{D_i}f^2(\mathbf{r},t)\\ &=k_0\left[f+\frac{1}{\tilde{A}}f^2\right]\ . \end{aligned} \tag{3.36}$$

Substituting this into the equation for $C(\bar{r},t)$, one finds

$$\begin{aligned} \frac{\partial C(\mathbf{r},t)}{\partial t}+k_0\left[1+\frac{C(\mathbf{r},t)}{\tilde{A}}\right]C(\mathbf{r},t)\\ =P+D_v\nabla^2\left[C-\frac{V_0\alpha}{2k_BT}C^2\right]\ . \end{aligned} \tag{3.37}$$

We have not studied this equation numerically, but considerations similar to the ones used above show that $C_s(0)$ obeys the equation

$$\frac{1}{\tilde{A}}C_s^2(0)+C_s(0)=\frac{\tilde{P}}{k_0}\ .$$

$P_{\rm th}$ is derived by setting $C_s(0)=C_{\rm th}$, which yields

$$P_{\rm th}/k_0=C_{\rm th}+\frac{1}{A}C_{\rm th}^2\approx\frac{1}{\tilde{A}}\left[\frac{k_BT}{V_0\alpha}\right]^2\ , \tag{3.38}$$

which, apart from a correction due to diffusive loss, is the same as Eq. (3.34).

Comparing these results for $P_{\rm th}$ with those of Sec. III A, in which the loss mechanism was taken to be linear,

TABLE I. Numerical values of frequently used parameters.

Vacancy coalescence energy V_0	0.15 eV
$\alpha=\Omega_i/\Omega_0$	10
Dislocation density ρ_d	10^{10} cm^{-2}
Activation energy for vacancy diffusion	0.8 eV
Activation energy for interstitial diffusion	0.12 eV
Diffusion constant prefactor	0.2 cm^2/sec
$k_0=\rho_d D_v$	7.27×10^{-5} sec^{-1} (at 300 K)
Diffusion length $L=(D_v/k_0)^{1/2}$	10^{-5} cm
Interstitial vacancy interaction parameter, $4\pi r_{iv}/\Omega_a$	6×10^{14} cm^{-2}
$\tilde{A}=\rho_d/(4\pi r_{iv}/\Omega_a)$	1.67×10^{-5}
$C_{\rm th}=\dfrac{k_B T}{V_0\alpha}$	0.0172 (at 300 K)

we note that the nonlinearity of the vacancy-interstitial loss mechanism affects the results rather strongly. The estimate of $P_{\rm th}/k_0$ in this section differs from that of Sec. III A by a factor $k_B T/V_0\alpha S(0)\tilde{A}$, whose numerical value for typical parameters given in Table I is 748.1 (for $R=4$). This large increase in $P_{\rm th}$ is understandable, as there is an additional loss mechanism now, which has to be compensated.

IV. NUMERICAL RESULTS

This section reports our numerical studies. We have a twofold aim. One is to study the actual temporal development implied by Eqs. (2.21) and (3.1), and check whether one has two kinds of behaviors as argued theoretically. The other is to check the accuracy of our theoretical estimates for the production threshold $P_{\rm th}$. All our numerical calculations have been done in one dimension, as the basic physical features can be well tested in one dimension. Since our model still lacks some realistic features, and its purpose is to elucidate the role of various competing processes, the effort to perform three-dimensional calculations does not seem justified at this stage. The numerical parameters used in the calculation are listed in Table I. Note that these parameters are just typical for nuclear materials, and do not correspond to any single material. In Table I we have also given values of some frequently used derived parameters such as k_0, A, $C_{\rm th}$, etc., for ready reference. For numerical calculations, the time is measured in units of k_0^{-1} and distance in unit of L.

For clarifying the role of various terms, the numerical calculations have also been done in two stages. In the first stage, we have studied Eq. (3.1), in which the recombination loss with the interstitials is approximated by a linear term. The temporal evolution of the concentration field is studied by switching on P at $t=0$, and taking the initial state to be one of thermal equilibrium. An explicit-difference method is employed to solve the equation. From numerical integrations, the existence of two types of solutions is clearly seen. For low values of P, the solutions quickly approach steady states, which are of the same qualitative form as those of the linear diffusion equation of Eq. (3.7). A typical steady-state solution is displayed in Fig. 1. Since the solution is symmetric around the center, only half the solution is shown. The

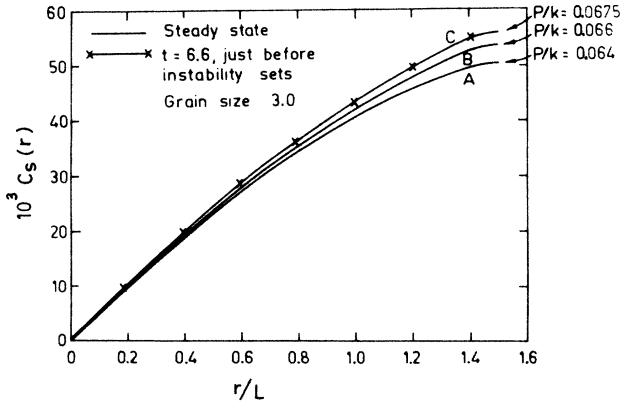

FIG. 1. Curves A and B show the concentration profiles of vacancies at two power levels, in the steady state. Curve C shows the concentration profile just before the instability set in. These concentration profiles are obtained by numerically integrating Eq. (3.1).

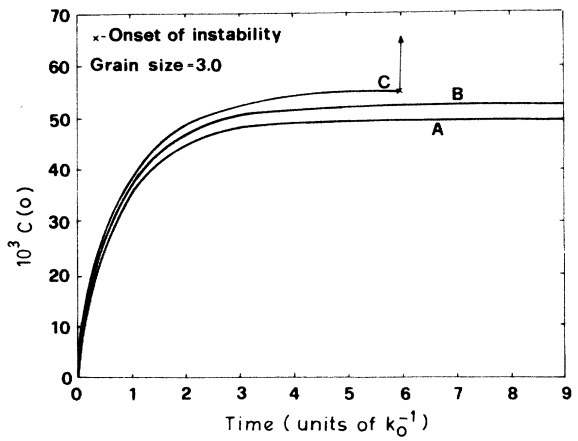

FIG. 2. The growth of vacancy concentration at the center of the grain according to Eq. (3.1) is plotted with time in units of k_0^{-1}. The curves A and B correspond to steady-state, while C corresponds to instability.

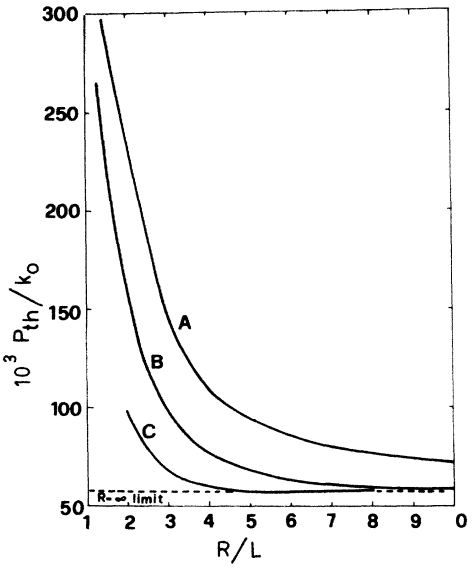

FIG. 3. Plots of $P_{th}/k_0 \times 10^3$ with grain size R/L according to numerical calculations and theoretical estimates. Curve C corresponds to numerical calculations, while curves A and B correspond to estimates according to Eqs. (3.19) and (3.23), respectively.

concentration throughout the grain grows monotonically towards the steady state. As P is raised, a certain stage is reached when the values of concentration at first approach seemingly the steady-state profile in a slow manner and then suddenly shoot to extremely large values at the grain center, signifying the instability. In Fig. 2, we show a plot of midpoint concentration, $C(0,t)$, for values of P below P_{th} and above P_{th}. We have also studied the size dependence of P_{th}, with a view to verify Eqs. (3.19) and (3.23). These results are shown in Fig. 3, in which the numerical results for P_{th}/k are shown with the theoretical prediction of Eqs. (3.19) and (3.23). Clearly our latter estimate of Eq. (3.23) is in closer agreement with the numerical results. For values of $R=5$, the theoretical estimates are within a few percent of the numerical values. For smaller values of R, the theoretical estimates are not so good, as for small R the approximations of neglecting $S-\bar{S}$ or $|\nabla F_T|/F_T$ are poor. However, from a practical point of view, this is not such a disadvantage, as the grain sizes practically encountered correspond to $R>5$ (i.e., grain size greater than 0.5 μm for our parameters).

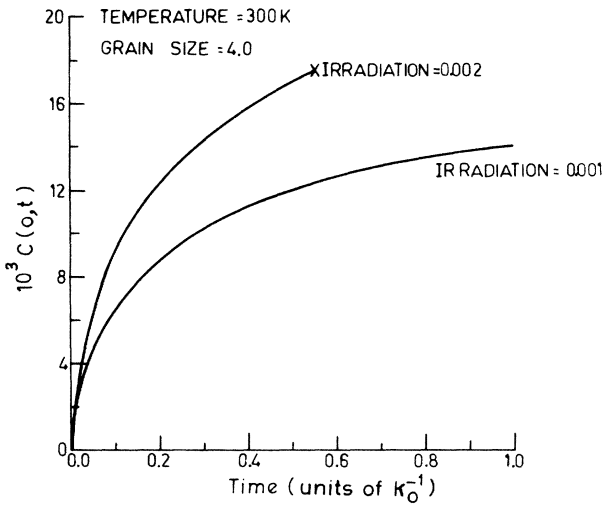

FIG. 5. The growth of concentration at the grain center at two production rates, one below P_{th} and the other above P_{th}.

We next report our numerical results on the complete Eq. (2.21). The calculations were carried out in the same way, except that one needs a greater precision. In this case, the truncation errors cause spurious instabilities,

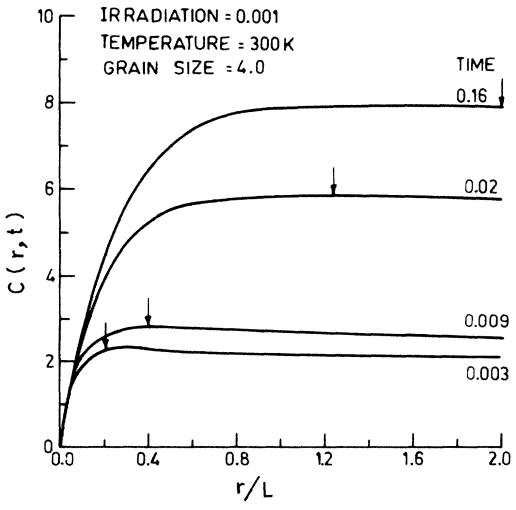

FIG. 4. Vacancy concentration profiles at various times, calculated according to Eq. (2.21).

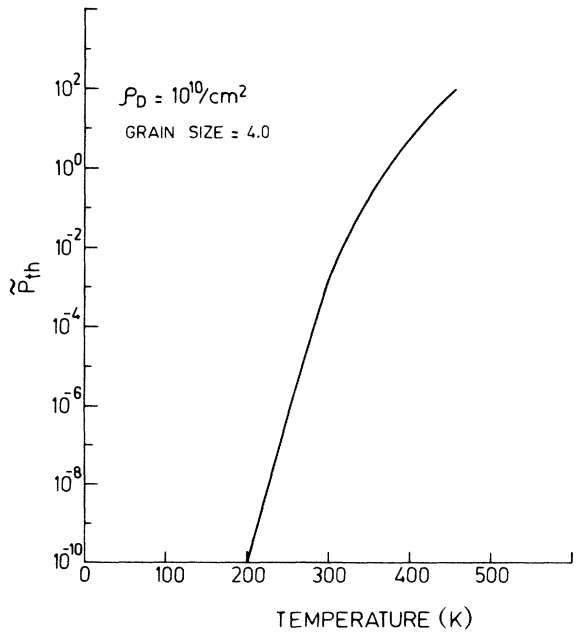

FIG. 6. The temperature dependence of P_{th} according to Eq. (3.38)

which are to be avoided. Again for small production rates P, one reaches a steady state. Some typical results are shown in Fig. 4. However, the approach to steady state has a new feature. Unlike the monotonic growth of the concentration profile found in the earlier case, here there is a faster increase in the concentration near the edges, initially, giving rise to a mild hump. This hump then travels towards the center, leading to the final profile. This is presumably due to the fact that the loss term due to interstitials is weaker near the edges initially. As before, as we raise P, an instability sets in, in the vicinity of the midpoint beyond a certain threshold. Figure 5 shows the growth of vacancy concentration at the grain center for two values of P, one below threshold and the other above it. The numerical value of $P_{\rm th}$ for $R=4$ was determined, by increasing P in steps of 10^{-4} and observing the breakdown of steady-state behavior. For $T=300$ K, $P_{\rm th}$ in this case was found to be 0.0013, which is gratifyingly close to the theoretical values of 0.001 29 calculated from the formula of Eq. (3.38). Note that Eq. (3.38) does not take into account the boundary loss correction factor of $S(0)$. Since $S(0)=1.83$ for $R=4$ inclusion of this factor spoils the comparison, which can still be regarded as satisfactory in view of the approximate treatment of nonlinearities. This points to the fact that the introduction of the boundary loss factor in Eq. (3.33) is not very good. Finally, in Fig. 6 we show the temperature dependence of $P_{\rm th}$ according to Eq. (3.38). One notes that this dependence is very rapid, which is largely due to the variation of the diffusion constant D_v with temperature.

V. CONCLUDING REMARKS

We have analyzed the conditions under which a gas of vacancies becomes unstable towards coalescence, leading to the formation of voids, causing their constant production under irradiation. Our model studies the competition between four kinetic processes, namely, the thermal diffusion of vacancies, their mutual attraction, their loss to various sinks in the material, and their production rate. The result is that there is a threshold production rate $P_{\rm th}$ only above which a spontaneous coalescence occurs. The theoretical predictions about $P_{\rm th}$ are made under two conditions. The first one, which is not too realistic in the present situation, treats the process of vacancy-interstitial recombination in a linear way. This calculation mainly serves the purpose of elucidating the competition between diffusion and the attractive interaction between the vacancies. The nature of diffusive instability giving rise to coalescence is particularly transparent in this situation, and this calculation also enables us to analyze the more complex situation to follow. In the second calculation the vacancy-interstitial recombination process is treated more realistically, by adopting an adiabatic approximation for the interstitial diffusion. The adiabatic approximation has a good justification in the present context, as vacancy diffusion is far slower than the interstitial diffusion. The theoretical estimates for $P_{\rm th}$ in the two calculations are quite different, but in both cases their agreement with the corresponding numerical calculations is very satisfactory; in fact, better than our expectation. Our theoretical formulas for $P_{\rm th}$ show explicit dependences on temperature, grain size, dislocation density, etc.

As far as void formation is concerned, our model can describe only the precoalescence stage. The description breaks down once the coalescence sets in, i.e., for $P > P_{\rm th}$. This is because the model contains no variables to describe the voids themselves. To describe the situation once such coalescence has occurred, one needs void variables and a description involving their coupling to vacancy concentration field, as has been done in some earlier work.[9–11] There are a few other features mentioned earlier in this paper which should be included to make the model more realistic.

Our general analysis applies to any population of objects subject to diffusive motion with short-ranged pairwise attractive forces.

ACKNOWLEDGMENTS

We are grateful to Dr. Kanwar Krishan for discussions and correspondence. We are also thankful to Dr. G. Venkataraman for inviting us to visit Reactor Research Centre, Kalpakkam, Tamidnadu, India, which led to this work. One of us (D.K.) also wishes to thank Professor Abdus Salam, Director of the International Centre for Theoretical Physics, Trieste, Italy, for hospitality at the Centre, where part of this work was done.

[1]M. W. Thompson, *Defect and Radiation Damage in Metals* (Cambridge, University Press, Cambridge, 1969), p. 11.

[2]*International Conference on Radiation Induced Voids in Metals*, edited by J. W. Corbett and L. Ianniello (unpublished).

[3]J. W. Corbett, J. C. Bourgoin, and C. Weigel, in *Radiation Damage and Defects in Semiconductors* (Institute of Physics, London, 1973), p. 1.

[4]K. Krishan and R. V. Nandekar, in Proceedings of Indo-German Seminar on Radiation Damage, edited by G. Venkataraman (unpublished), p. 156.

[5]H. Ullmaier and W. Schilling, in *Physics of Modern Materials*, (International Atomic Energy Agency, Vienna, 1980), Vol. 1, p. 301.

[6]G. W. Greenwood and J. E. Harris, Acta Metall. **13**, 936 (1965).

[7]L. M. Brown and W. M. Stabbs, Philos. Mag. **23**, 1201 (1971).

[8]J. R. Rice and D. M. Tracey, J. Mech. Phys. Solids **17**, 201 (1969).

[9]A. D. Brailsford and R. Bullough, J. Nucl. Mater. **44**, 121 (1972).

[10]R. Bullough, B. L. Eyre, and K. Krishan, Proc. R. Soc. London **346**, 81 (1975).

[11]K. Krishan and R. V. Nandekar, Pramana **12**, 607 (1979).

[12]K. C. Russell, Acta Metall. **26**, 1615 (1978).

[13]C. F. Clement and M. H. Wood, J. Nucl. Mater. **89**, 1 (1980).

[14]S. Sharafat and N. M. Ghoniem, J. Nucl. Mater. **122**, 531

(1984).
[15]G. Martin, Philos. Mag. **32**, 615 (1975).
[16]S. J. Rothman, in *Phase Transformations during Irradiation*, edited by F. V. Nolfi, Jr. (Applied Science Publishers, London, 1983), p. 189.
[17]R. Sizmann, J. Nucl. Mater. **69&70**, 386 (1978).
[18]F. W. Young, J. Nucl. Mater. **69&70**, 310 (1978).